Published by :
http://www.ijert.org

International Journal of Engineering Research & Technology (IJERT)
ISSN: 2278-0181
Vol. 14 Issue 08, August - 2025

Direct Multi-Objective Optimization of All-on-Four Implant Parameters Across Three Saudi Jawbone Morphologies

Talei Al-Matrafi, Khaled Ibrahim, Ghadeer Basunbul,
Mohamed Ashour Ahmed, Ammar Melaibari

Department of Mechanical Engineering, Faculty of Engineering, King Abdulaziz University, Jeddah 21589, Saudi Arabia
Department of Faculty of Dentistry, King Abdulaziz University, Jeddah 21589, Saudi Arabia
Prosthodontics department, Faculty of Dentistry, Taif University, Taif 21589, Saudi Arabia

Abstract:
Purpose: This study uses finite-element analysis (FEA) to optimize the all-on-four dental implant design, aiming to minimize stress on the cortical bone across different Saudi mandible shapes.
Methods: Three parametric 3D finite-element models, representing the average dimensions of oval, tapered, and square Saudi edentulous mandible shapes, were developed[1]. A 50 N occlusal load was applied to the distal implants [2], and the resulting maximum Von Mises and maximum principal stresses on the cortical bone were measured..

Results: Finite-element analysis optimized All-on-Four implants for three Saudi mandible shapes (square, oval, tapered), successfully maintaining cortical bone stress below 3 MPa. The square shape showed the lowest stress (2.1 MPa) and the tapered the highest (2.7 MPa). Optimal design parameters were identified as 4.0–4.4 mm implant diameters, ~45° posterior angulation, and ~15° anterior angulation, providing key guidelines for biomechanical safety

Conclusion: The square mandible exhibited the best biomechanical performance due to its larger cortical support area, which distributes stress more evenly, while the tapered shape performed worst as its narrow geometry increases bending moments and stress concentrations. Optimization consistently identified key parameters to minimize stress: implant diameters of 4.0–4.4 mm reduce contact pressure, and a posterior angle of ~45° optimizes load sharing. The anterior implant angle had minimal impact. This study highlights that cortical bone stress distribution in All-on-Four treatments is primarily influenced by mandibular shape fit, implant placement along the curvature, posterior implant inclination, and implant diameter.

Keywords: **All-on-4, Dental implants, Edentulous mandible, Multiple-Objective, Optimization, Stress.**

INTRODUCTION

In the late 1990s, full-arch rehabilitation went through a huge transformation with the concept of the All-on-Four dental implant system which was initially introduced by Dr. Paulo Malo [3]. It was introduced as a minimally invasive and effective replacement to conventional implant techniques. The concept was to place four angled implants in an edentulous jaw for supporting the fixed prosthesis usually without the requirement of bone-grafting. Moreover, the said technique increased the implant stability and reduced the surgical complications by utilizing the present bone system of higher bone density areas, for instance, the mandible or anterior maxilla [3], [4].
Later, in 2003, a team of researchers presented the All-on-Four method due to the low availability of residual alveolar bone, in some cases of edentulous patients cause difficulty in using implants for fixed prosthesis[5]. The All-on-Four dental implant consists of a superstructure, involving two vertical straight implants in the anterior region of the jaw, and two long inclined implants in the posterior region to minimize the effect of the cantilever length [6], [7], [8]. Figure 1 presents a practical explanation of the implementation of the All-on-Four implant in which the four implants are placed in the front portion of the jaw among which two in front follow the curvature of the jaw, and the two in back are angled from 0^0 – 45^0 angles. Long-term research indicates that this strategy has success rates ranging from 92.2 – 100%, identifying the All-on-Four idea as a significant advancement in dental repair and restoration [9].

International Journal of Engineering Research & Technology (IJERT)
ISSN: 2278-0181
Vol. 14 Issue 08, August - 2025

Figure 1: Implementation of All-on-Four dental implant system [3].

The All-on-Four dental treatment presents advantages that it is a compelling option for dental professionals as well as individuals. Firstly, it avoids the need for intricate surgical procedures like nerve relocation or sinus augmentation, which are usually required when using traditional dental implants. Secondly, as stated earlier, the All-on-Four system reduces recovery time and total treatment costs by eliminating the need for bone grafting. Finally, since the impressive strategy of implant positioning, the All-on-Four design guarantees improved biomechanics, thus making prosthesis care simpler and providing the patient with instant functional and cosmetic benefits [8] . However, the All-on-Four dental implant system has some limitations which include tight restrictions on prosthetic cantilever extensions, implantation placement cannot always be done arbitrarily or freely and, the process is extremely technique-sensitive that requires complex pre-surgery preparations, for example the use of surgical splints and CAD/CAM. Furthermore, patients with specific physical characteristics or advanced gum disorders have a problem with this All-on-Four surgery technique[10].

The field of dental implant systems has evolved with the advent of patient-specific modeling, which involves advanced imaging and computational simulations to custom-tailored dental implant treatment plans. This method acknowledges that anatomical and physiological differences across patients, more specifically relating to the jawbone geometry and bone density, are capable of greatly impacting the implant success and long-term biomechanical performance. Patient-specific modeling is particularly critical in populations with distinct craniofacial features, for instance, the Saudi population, where regional skeletal variations must be considered for optimized outcomes [11], [12], [13], [14].

The shape of the mandible plays a critical role in facial aesthetics and dental occlusion (how the upper and lower teeth fit together). Understanding the most common mandibular arch forms is essential for orthodontists and dentists when planning treatment for their patients. The common mandibular arch forms[8], [15], [16] are depicted in Figure 2, and five dental arch forms for normal occlusion in the mandible and maxilla[17] are illustrated in Figure 2 which include:

1- Tapered: Triangular-shaped arch with a wider posterior segment and narrow anterior segment.
2- Square: Quadrilateral-shaped arch with nearly equal width throughout.
3- Ovoid: Oval-shaped arch with a rounded anterior segment and gradually tapering posterior segments.
4- Catenary: Arch form 1.

International Journal of Engineering Research & Technology (IJERT)
ISSN: 2278-0181
Vol. 14 Issue 08, August - 2025

5- Halfway between the ellipse and U-shaped arch: Arch form 2.
6- Tudor: Arch form 3.
7- Tapered equilateral: Arch form 4.
8- Quadrangular: Arch form 5.

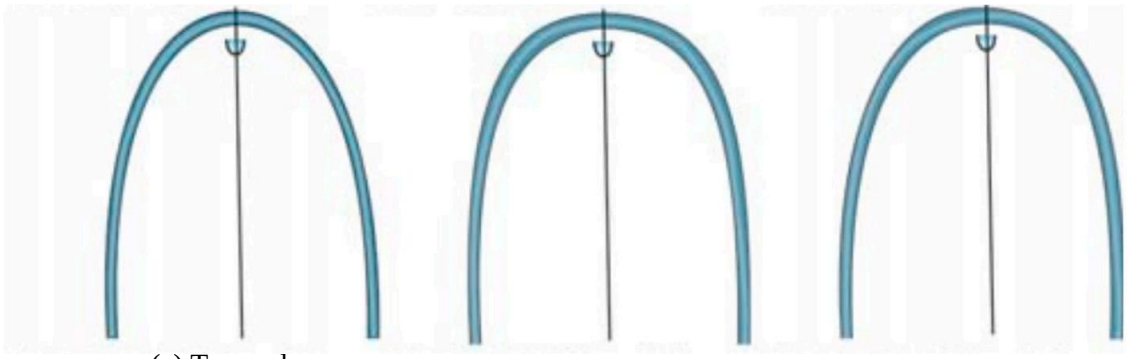

(a) Tapered (b) Squared (c) Ovoid

Figure 2. : Common mandibular arch forms [9], [41], [65]

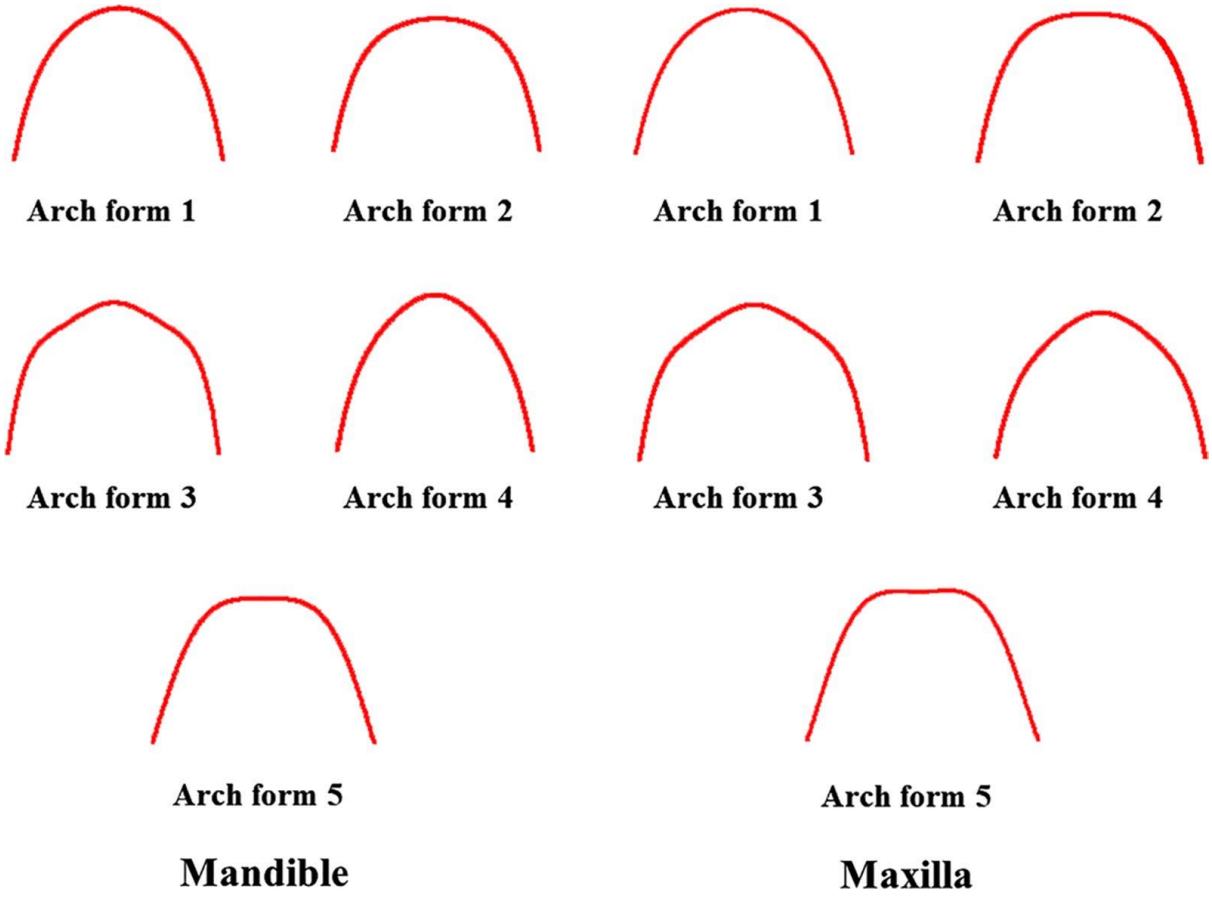

Figure 2. : Graphic representations of the five dental arch forms for normal occlusion in the mandible and maxilla [17].

Japanese mandibular model demonstrated by Takeshi et al. [2], that an All-on-4 configuration with two parallel anterior and two angled posterior implants resulted in lower cortical bone stress than those for configurations with six parallel implants in Japanese mandibular models.

In Saudi Arabian people, the most common form is ovoid (48.4%) followed by square arch form (30.2%) and tapered (21.4%). No significant difference existed between males and females regarding the mandibular arch form. Comparing arch-perimeters, no significant difference existed between either gender in inter canine width and depth. The most compatible archwire to the population's upper dental arch is the Ortho organizer oval arch. While Dentaurum, the Tensic-ideal arch is the most compatible archwire to the lower dental arch[18] . The dental

International Journal of Engineering Research & Technology (IJERT)
ISSN: 2278-0181
Vol. 14 Issue 08, August - 2025

arch dimensions of Saudi Arabians may differ slightly from other populations due to genetic and environmental factors. The maxillary arch dimensions of Saudi Arabian people are 36 to 40 mm (intercanine) 58 to 62mm (intermolar) as width dimensions, and 45 to 50 mm as depth. Moreover, the dimensions of the mandibular arch are 35 to 39 mm (intercanine) 55 to 59 mm (intermolar) as width dimensions, and 35 to 40 mm as depth[19]. The difference in dental arch dimensions between males and females was conducted[20]. Munther A. Ali et al.[21] discovered mandibular clinical arch shapes and dimensions in the Iraqi population, comparing distribution across Arabs and Kurds and examining the link with malocclusion classes. A total of 1005 research models were gathered, with arch morphologies ranging from ovoid (47%), tapered (36.2%), to square (16.8%), with no significant difference between Arabs and Kurds. In order to determine an initial reference for the selection of artificial teeth in Yemeni adults, Samar et al[22] assessed the dental arch dimension (length, width, and height) as well as facial measurements, such as bizygomatic width (BZW), inner-canthal width (ICW), mouth width (MW), and inter-alar width (IAW). In addition to evaluating the correlation between these facial measurements and dental arch width (inter-first premolar width (I1PW), canine width (CW), and inter-first molar width (I1MW)). Eighty people with symmetrical features and normal class I occlusion, aged 20 to 35, were enrolled in the research (40 men and 40 women). For every person, a mandibular and maxillary stone cast was created. A computerized caliper was used to measure the dimensions of dental casts and face measures, such as ICW, BZW, IAW, and MW. The SPSS software was used to analyze the gathered data. For every measurement, descriptive statistics were created. An independent-sample t-test was used to examine differences between males and females, with p-values of less than 0.05 being regarded as significant. There was also a Pearson connection coefficient between the breadth of the dental arch and the face dimensions. Finally, they found that the appropriate size for the prosthetic teeth in the anterior maxillary arch can be ascertained by the ICW. However, in Yemeni communities, the other face parameters (IAW, BZW, and MW) cannot be used in the selection of prosthetic teeth. Aljayousi et al[23] explained and clarified the mandibular and maxillary arch shapes in the Jordanian people. They examined 289 females and 231 males (mean age of 15.4±1.02 years). The prevalence of the catenary arch form was 41.2% and 47% ($p < 0.01$) Of the mandible and maxilla arch forms, respectively. Archly, they found that the most common arch shape in Jordanian people was the catenary form, which was followed by the broad elliptical form. The other types had occurred less often, which included the tapering equilateral, quadrangular, and Tudor arch. Simran et al[24] determined sexual dimorphic traits in the arch patterns of Nepalese people based on tooth arrangement patterns and the maxillary and mandibular arches using Euclidean Distance Matrix Analysis (EDMA). They examined 96 Nepalese people (18 – 25 years). The EDMA objectively confirmed the occurrence of tapering arch forms in Nepalese females and square arch forms in Nepali men with references to the landmarks confirming such a change.
Dental implant biomechanics combines heterogeneous materials (metallic implants, prosthetic superstructures, and anisotropic bone) and complex loading; therefore, choosing appropriate mechanical metrics is essential for meaningful design, optimization, and clinical guidance. In this study we use a dual optimization objective (minimizing both von Mises stress and maximum principal stress [25]) when optimizing all-on-four implant parameters across three representative Saudi jawbone morphologies (square, oval, tapered). The rationale for the two metrics, their physical meaning, and their specific relevance to the implant–bone system are summarized below.
Von Mises stress is commonly used as a single-value indicator of the severity of multiaxial stress in FEA. Therefore, Von Mises stress is used to provide an overall scalar measure of combined stress effects (including shear and deviatoric components) in the bone surrounding dental implants which can be useful for comparing designs or loading conditions. In short, von Mises is an effective consolidated metric for multi-axial stress concentration and load-sharing trends produced by geometry and angulation choices[26].
Maximum principal stress is the largest normal stress acting on a principal plane (a plane where shear stress is zero). It identifies the direction and magnitude of the maximum tensile (or compressive) normal stress in a body under multiaxial loading and is widely used to predict brittle or tensile-driven failure modes[27].
Cortical bone shows markedly different behavior in tension versus compression — it is generally stronger under compression and more vulnerable under tensile loading and fatigue, and failure often initiates on the tensile side under bending loads. Consequently, maximum principal stress (particularly the tensile principal stress) is a biologically and mechanically meaningful predictor of locations at risk of microdamage or crack initiation in cortical bone surrounding implants. Using principal stress as an evaluation metric therefore captures failure modes that von Mises (a ductile-material based scalar) can under-represent for brittle or anisotropic tissues[28].

International Journal of Engineering Research & Technology (IJERT)
ISSN: 2278-0181
Vol. 14 Issue 08, August - 2025

MATERIAL AND METHODS

Stage I: Comparison design and stress measurement on the cortical bone with Takeshi et al. [2] (Japanese model)

The 3D mandibular model, which incorporates both cortical and cancellous bone layers along with the complete All-on-4 implant system (superstructure, abutments, and four implants), is developed based on the parametric framework established by Takeshi et al.[2]. Key geometric parameters from the reference study are systematically replicated in the new design model while maintaining identical force application points, meshing protocols, and boundary conditions during the comparative analysis phase.
The stress distribution analysis conducted using the ANSYS Workbench demonstrates consistent cortical bone-loading patterns across all tested posterior implant angulations (0°, 15°, 30°, and 45°), as illustrated in Figure 3. The results exhibit a strong correlation with reference data, particularly with the stress magnitude and distribution characteristics. This validation confirms the ability of the model to accurately replicate biomechanical behavior under varying implant configurations while maintaining anatomical fidelity.

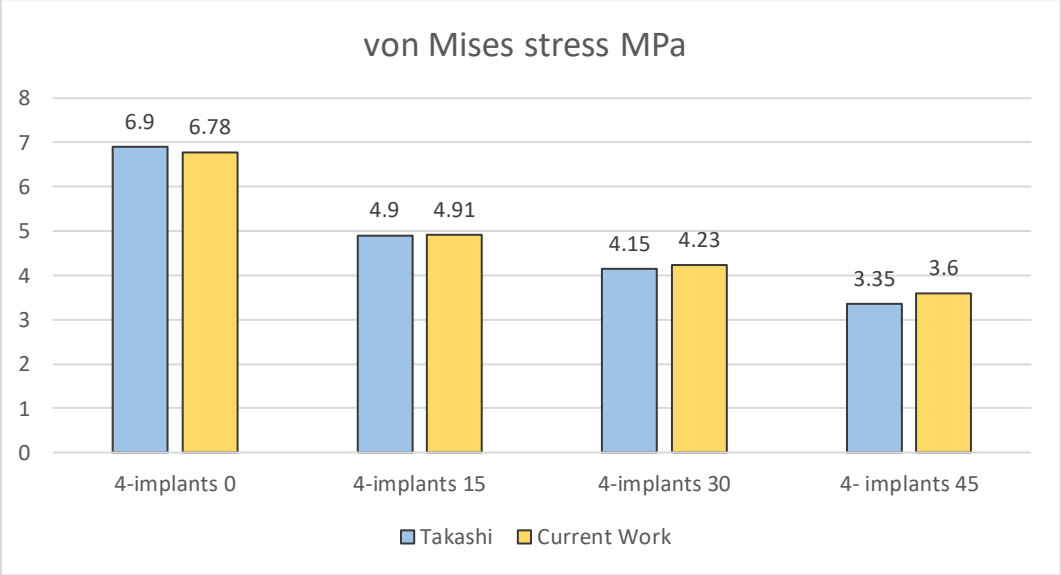

International Journal of Engineering Research & Technology (IJERT)
ISSN: 2278-0181
Vol. 14 Issue 08, August - 2025

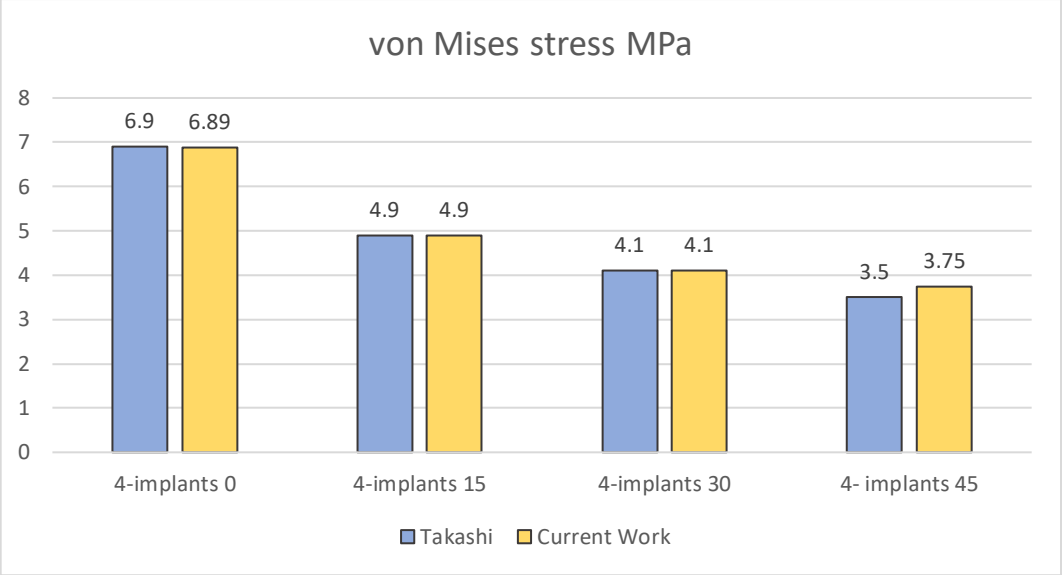

Figure 3 : Comparison stress distribution under loading based on Takeshi (Takahashi et al [2]) conditions B for anterior implant 13 and 15 mm and this paper.

Stage II: Design optimization and stress measurement on cortical bone for Saudi Models Model geometry and parameterization

A three-dimensional finite-element model was created in ANSYS DesignModeler and parameterized so implant geometry and placement could be varied automatically during optimization. The model contains the three main bodies used throughout the study: implant, cortical bone, and cancellous bone. Four implants are present in the prosthesis (an all-on-four configuration). Three jaw geometries were generated to represent the study population:

- Model 1 (Square)
- Model 2 (Oval)
- Model 3 (Tapered)

The three geometries were derived from a statistical model based on the jaw classification dataset cited in the study source[18]. A normal distribution (mean ± 2·standard deviations) Figure 4 was used to select representative dimensional values Table 1; these dimensions were then used to construct the three jaw shapes and the prosthesis shape used in the CAD models[29].

Table 1: The Saudi mandible curvature dimensions for Model 1 (Square), Model 2 (Oval), and Model 3 (Tapered).

	M1 Curve		M2 Curve		M3 Curve	
	X	Y	X	Y	X	Y
L	-27	0	-29	0	-31.25	0
L	-24.214	16.6957143	-27.09	12.3657143	-29.966	8.03571429
L	-20.278	32.8937143	-23.06	29.6857143	-25.842	26.4777143
L	-11.96	51.6737143	-14.02	49.2657143	-16.08	46.8577143
L	0	55.2857143	0	55.2857143	0	55.2857143
R	11.96	51.6737143	14.02	49.2657143	16.08	46.8577143
R	20.278	32.8937143	23.06	29.6857143	25.842	26.4777143
R	24.214	16.6957143	27.09	12.3657143	29.966	8.03571429
R	27	0	29	0	31.25	0

International Journal of Engineering Research & Technology (IJERT)
ISSN: 2278-0181
Vol. 14 Issue 08, August - 2025

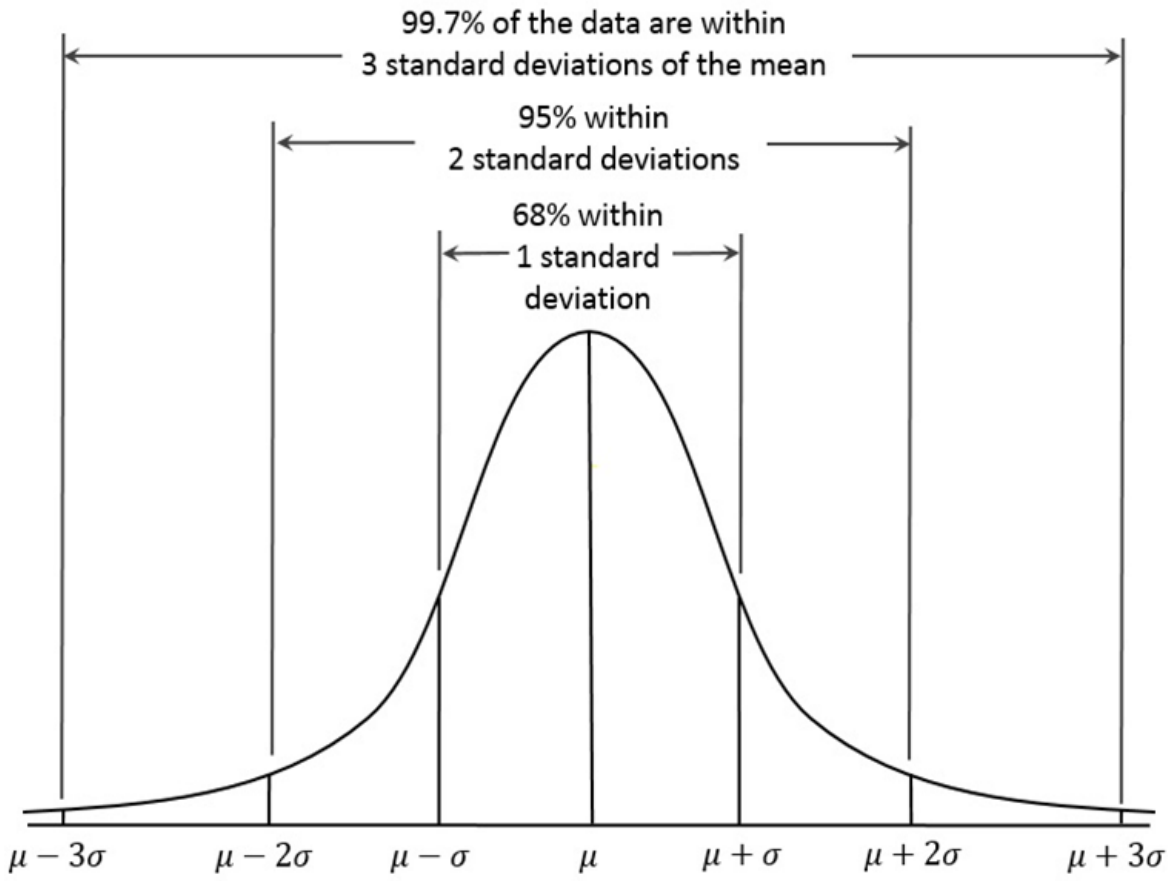

Figure 4: Standard deviations and normal distribution.

Geometry parameterization includes four variables, out of which three are accessible to the direct optimizer:

1. Implant diameter
2. Anterior implant position angle
3. Posterior implant top face angle
4. Posterior implant bottom face angle – Fixed variable not used in optimization

SAUDI JAW BONE TYPES

The models are classified into three Saudi Jaw bone types namely, Square, Oval, and Tapered [18]. The geometry classification of the models is as follows Figures 5-7:

International Journal of Engineering Research & Technology (IJERT)
ISSN: 2278-0181
Vol. 14 Issue 08, August - 2025

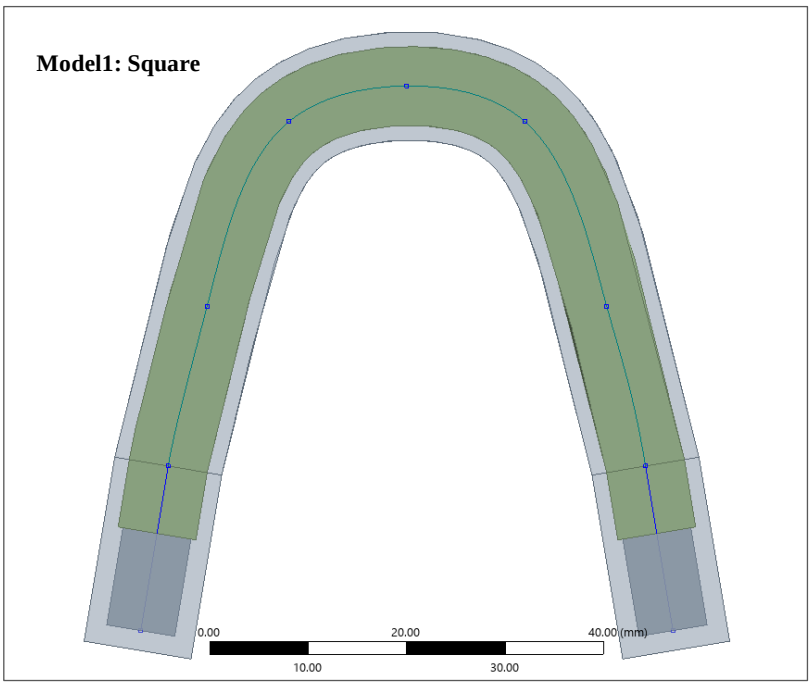

Figure 5: The Saudi square model (Model 1).

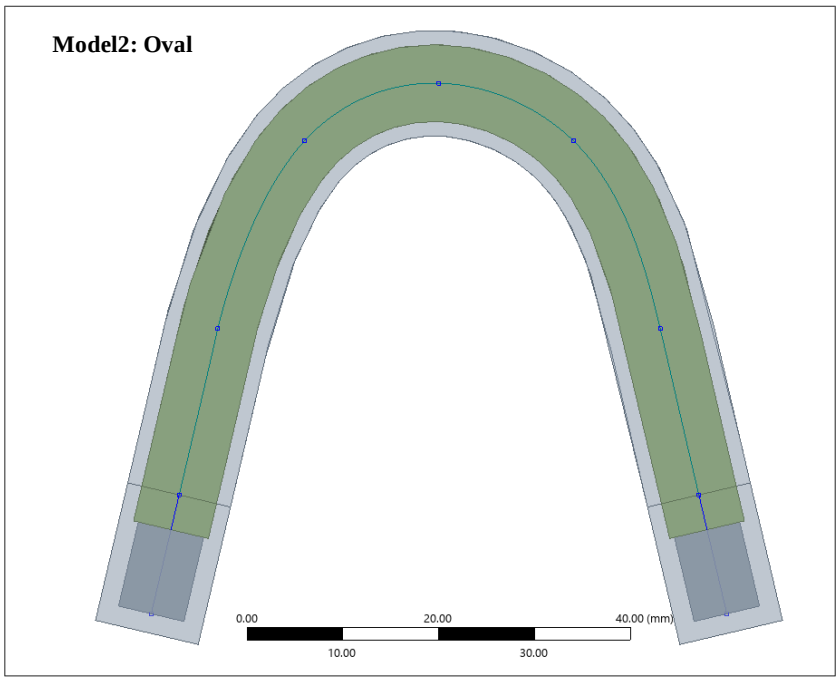

Figure 6: The Saudi oval model (Model 2).

International Journal of Engineering Research & Technology (IJERT)
ISSN: 2278-0181
Vol. 14 Issue 08, August - 2025

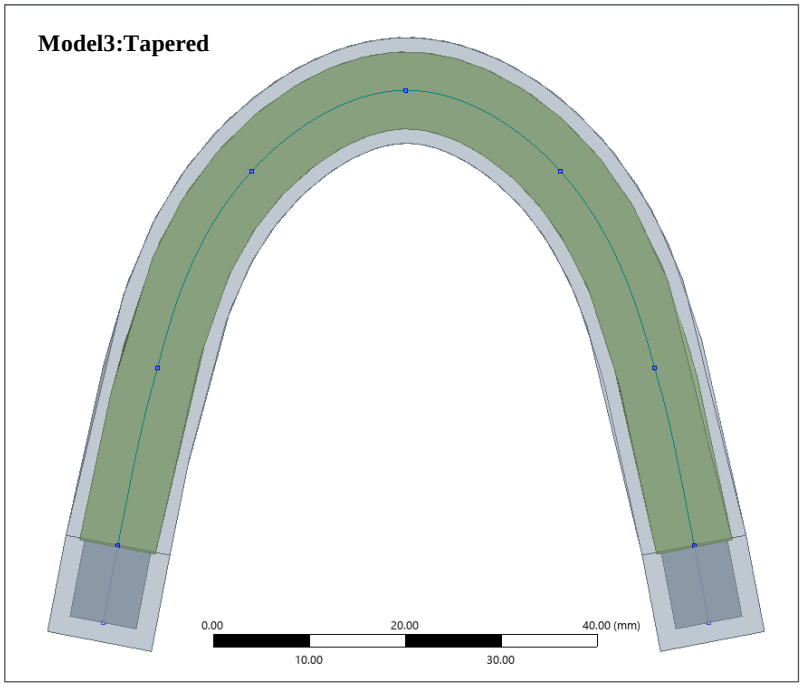

Figure 7: The Saudi Tapered model (Model 3).

The implant diameter controls the implant cross-section. There are a total of four implants. The anterior implants are vertical with no inclination, and the posterior implants are inclined. There are a total of three angles that control both the position and inclination of the implants. A single angle controls the anterior implant position relative to the center of the jaw arc. Two angles control the top and bottom faces of the posterior implant, thereby controlling the position as well as the inclination of the posterior implant. The posterior implant bottom face angle is kept fixed and is not used as an optimization parameter. The posterior implant's position and inclination is controlled by adjusting (via optimization) the posterior implant's top face angle.

The pre-optimization (baseline) parameter values were:

- Anterior implant angle = 15°
- Posterior top angle = 55°
- Posterior bottom angle = 35°
- Implant diameter = 4.0 mm

All three jaw models used the same baseline parameter set prior to optimization.

MATERIALS

Material properties for cortical bone, cancellous bone, and the implant material were assigned using linear elastic isotropic models[2] and are reported below Table 2 [28].

International Journal of Engineering Research & Technology (IJERT)
ISSN: 2278-0181
Vol. 14 Issue 08, August - 2025

CONTACTS AND INTERFACE ASSUMPTIONS

Contacts were modeled consistently across the three geometries:

- Cancellous–cortical bone: bonded contact.
- Implant–cancellous bone: bonded contact.
- Implant–cortical bone: frictional contact with a friction coefficient of 0.3 (model setting: adjust-to-touch).

These contact definitions were chosen to reflect common practice in dental FEA studies: bonding the implant to cancellous bone simplifies internal load transfer assumptions, while a frictional interface at the cortical surface captures the limited sliding and shear transfer expected at the implant neck.

Table 2: The Material properties for cortical bone, cancellous bone, and the implant material[2].

Body	**Density ($kg \cdot m^{-3}$)**	**Young's modulus (MPa)**	**Poisson's ratio**
Cortical bone	2000	20000	0.3
Cancellous bone	1000	2000	0.4
Implant (Superstructure)	4620	1.085e+05	0.34

Note: Bonded contacts are conservative and tend to increase absolute stress values; however, the use of identical contact settings across all three models preserves relative comparisons and optimization trends. Although bonded contacts do overestimate stresses slightly, they would provide a greater safety margin in doing so when designing dental implants. It is also commonly taken up practice to use bonded contact in dental FEA for such cases albeit a simplification.

LOADING AND BOUNDARY CONDITIONS

A vertical load of 50 N was applied [2]to one side of the prosthetic structure to represent a localized bite/occlusal loading condition used consistently across all models. Boundary conditions for fixed support were applied to represent the anatomical support of the mandible; supports were identical for all three models to ensure comparability of results.

MESH AND DISCRETIZATION

A uniform global mesh size of 0.001 m (1.0 mm) was used for all models to ensure consistent discretization between geometries.

Automatic measuring tools in software packages such as ANSYS Workbench often use tetrahedral elements due to their versatility and because tetrahedral elements are capable of capturing a high degree of geometric non-linearity. In this study, tetrahedral elements were chosen for the discretization. Tetrahedral elements are widely used in FEA because they adapt easily to complex geometries such as bones and dental implants, where surfaces are highly curved and irregular. They are also automatically generated by most meshing algorithms, making them efficient to implement.

For our case, the use of tetrahedral elements was especially suitable because the bone and implant structures are highly irregular. Hexahedral elements, while accurate for simple geometries, are difficult to generate for complex shapes. Tetrahedral meshing allowed us to capture the fine details of the implant–bone interface, which is critical for evaluating load transfer and stress distribution in biomedical applications Figure 8.

In short, tetrahedral meshing is robust for complex, highly curved anatomical geometries and supports automatic, reproducible mesh generation. This approach is commonly adopted in implant FEA studies [29].

International Journal of Engineering Research & Technology (IJERT)
ISSN: 2278-0181
Vol. 14 Issue 08, August - 2025

To identify implant design and placement parameters (implant diameter, anterior implant position, posterior implant inclination) that minimize both von Mises and maximum principal stresses in the cortical jawbone for three representative jaw shapes (square, oval, tapered), using direct optimization in ANSYS.

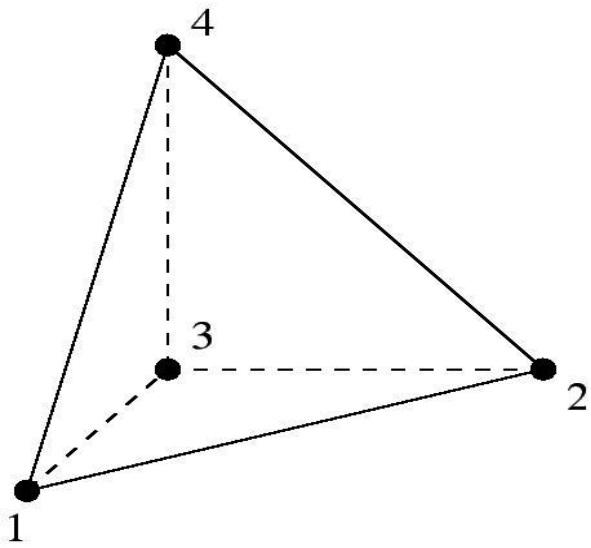

Figure 8: The tetrahedral elements used to capture the fine details of the implant–bone interface.

The mesh quality was checked and a mesh convergence study was performed to ensure result independence from discretization.

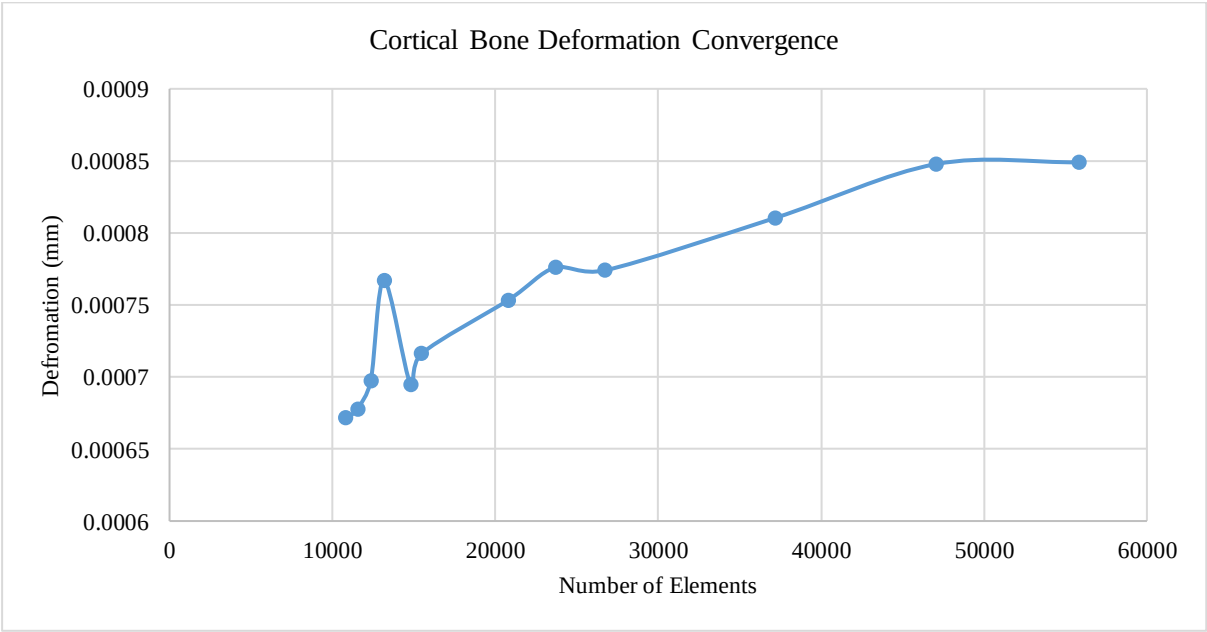

Figure 9: The mesh convergence study.

International Journal of Engineering Research & Technology (IJERT)
ISSN: 2278-0181
Vol. 14 Issue 08, August - 2025

To ensure the reliability of the results, a mesh convergence study was conducted. In this study, the number of elements was progressively increased, and the resulting deformation in the cortical bone was recorded Figure 9.

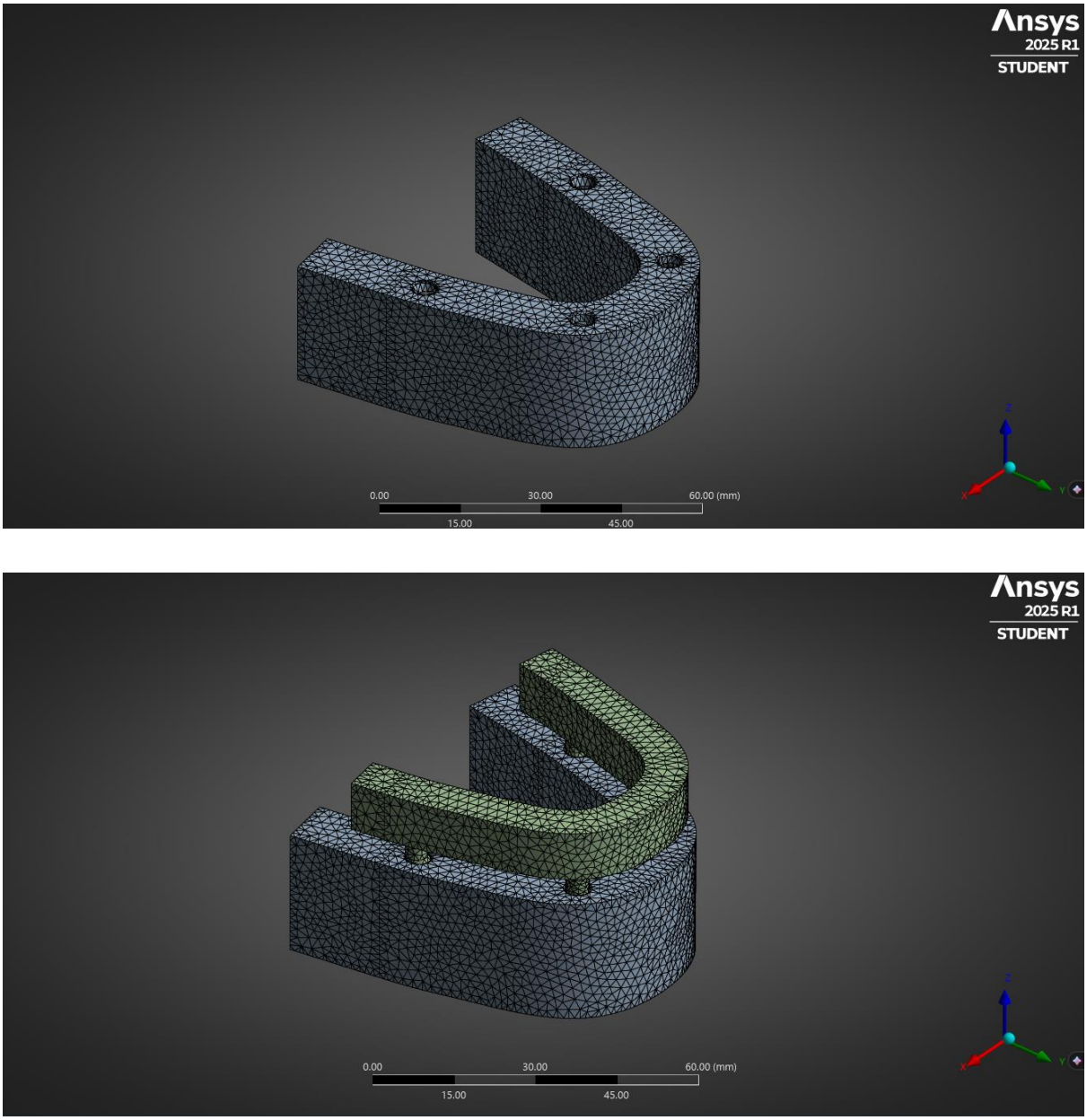

Figure 10: Model meshing by tetrahedral element.

The convergence graph shows that at very coarse meshes (lower element numbers), the deformation values fluctuate noticeably, indicating numerical inaccuracy. As the number of elements increases, the deformation values begin to stabilize. Beyond ~47,000 elements, the deformation values converge, meaning that further refinement produces negligible change in results. This good convergence behavior, deformation values approaching a stable solution, confirms that the mesh density chosen is sufficient to ensure accuracy without unnecessary computational cost. For the final model, an element size (1.0 mm giving 55838 elements) was chosen based on this convergence point, balancing accuracy with computational efficiency Figure 10.

International Journal of Engineering Research & Technology (IJERT)
ISSN: 2278-0181
Vol. 14 Issue 08, August - 2025

DUAL OPTIMIZATION STRATEGY

Table 3: The optimization parameters.

Name	Lower Bound	Upper Bound
Posterior implant position angle(Degree)	35	60
Anterior implant position angle(Degree)	13.5	16.5
Implant diameter (mm)	3.6	4.4

Table 4: The Optimization Objectives.

Optimization Objective	Target
Equivalent Von Mises stress (MPa)	Minimize the maximum stress on cortical bone
Maximum Principal Stress (MPa)	Minimize the maximum stress on cortical bone

The implant-bone system loading produces both shear/distortional and tensile normal stress components, thus no single scalar fully characterizes all clinically relevant risk modes. Previous finite-element investigations of dental prostheses and All-On-Four concepts routinely report both von Mises and principal stresses (or explicitly compare equivalent vs. principal stresses) because each highlights different aspects of mechanical risk (implant yielding, abutment stress, shear-dominated regions, vs. tensile-prone cortical bone zones). Reporting and minimizing both metrics therefore improves the clinical relevance of an optimization and reduces the chance of a design that is "optimal" by one metric but harmful by the other.

- Von Mises stress is highly sensitive to shear components so at bone-implant interfaces, significant shear develops even when normal stresses are low. There is constrained deformation when the cortical bone is "sandwiched" between stiff implants and softer cancellous bone. This constraint generates shear stress that elevates Von Mises Stress without significantly increasing Max principal stress. It's important to cater to shear stress as sharp geometric features, localized shear distortion occurs while tensile or compressive stress remains moderate.
- Maximum Principal Stress is important where failure is governed by maximum tensile stress (or compressive stress) causing crack propagation. Brittle materials such as bone have low tolerance for tensile stress concentrations so a geometry optimized for low max tensile σ_1 will be more resistant to fracture.

A multi-objective formulation enforces a balanced trade-off so that final parameter choices (implant diameter, anterior/posterior positioning and inclination) reduce both mechanical risks simultaneously. Multi-objective numerical optimization methods (including genetic algorithms like MOGA) have been successfully applied to dental implant geometry and prosthetic design for this purpose.
Jawbone geometry strongly controls load paths, lever arms, and the cortical envelope available to accept implant loads; therefore the optimal balance between von Mises and principal stresses will depend on jaw shape (square, oval, tapered). By casting the problem as a dual-objective direct optimization (MOGA) and using consistent loading, contact, and mesh assumptions across models, the study explicitly seeks parameter (Table 3 and 4) sets that minimize both von-mises (equivalent) and tensile (principal) risks across the morphologies. This approach aims to produce clinically useful recommendations (for implant diameter and posterior inclination) that are not biased toward a single failure mode and that remain comparable across jaw types.

RESULTS

Optimization Study Candidate Points
The candidate points from the optimization study for each model are as follows:

International Journal of Engineering Research & Technology (IJERT)
ISSN: 2278-0181
Vol. 14 Issue 08, August - 2025

Table 5: Candidate points identified for Model 1 optimization.

Candidate Points	Posterior implant position angle(Degree)	Anterior implant position angle(Degree)	Implant diameter (mm)	Von Mises Maximum	Maximum Principal Stress
Candidate point 1	47.699	14.163	4.355	2.149	1.384
Candidate point 2	47.110	14.372	4.383	2.031	2.003
Candidate point 3	51.575	14.892	4.353	2.2429	2.550

Table 6: Candidate points identified for Model 2 optimization.

Candidate Points	Posterior implant position angle(Degree)	Anterior implant position angle(Degree)	Implant diameter (mm)	Von Mises Maximum	Maximum Principal Stress
Candidate point 1	44.519	15.572	3.988	2.431	1.664
Candidate point 2	47.625	14.406	4.295	2.6679	1.675
Candidate point 3	52.625	14.663	4.098	2.748	1.840

Table 7: Candidate points identified for Model 3 optimization.

Candidate Points	Posterior implant position angle(Degree)	Anterior implant position angle(Degree)	Implant diameter (mm)	Von Mises Maximum	Maximum Principal Stress
Candidate point 1	45.662	14.857	4.374	2.700	2.053
Candidate point 2	45.653	14.811	4.265	2.706	3.099
Candidate point 3	45.662	16.258	4.264	2.881	2.239

International Journal of Engineering Research & Technology (IJERT)
ISSN: 2278-0181
Vol. 14 Issue 08, August - 2025

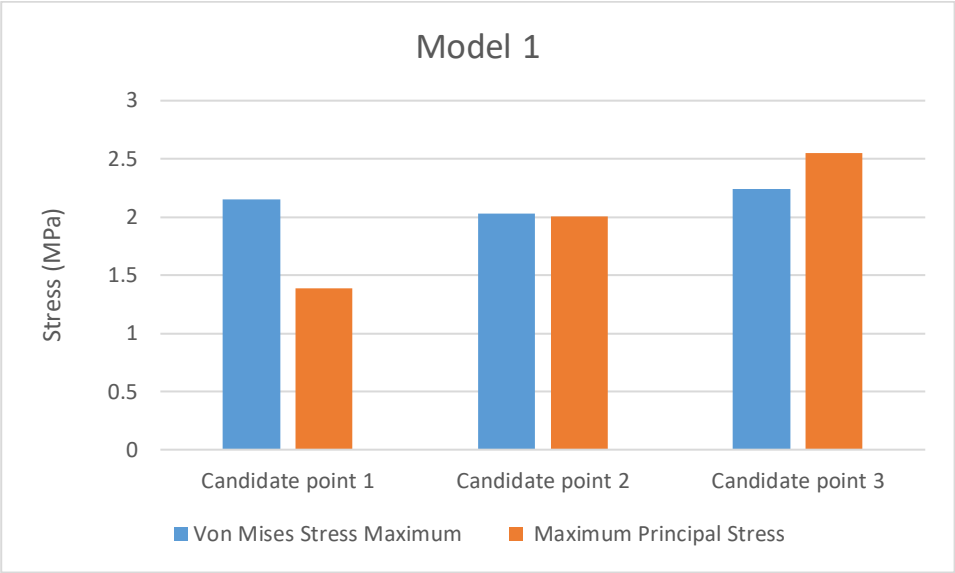

Figure 11: Comparison results Von Mises stress and Principle stress on cortical bone of Model 1.

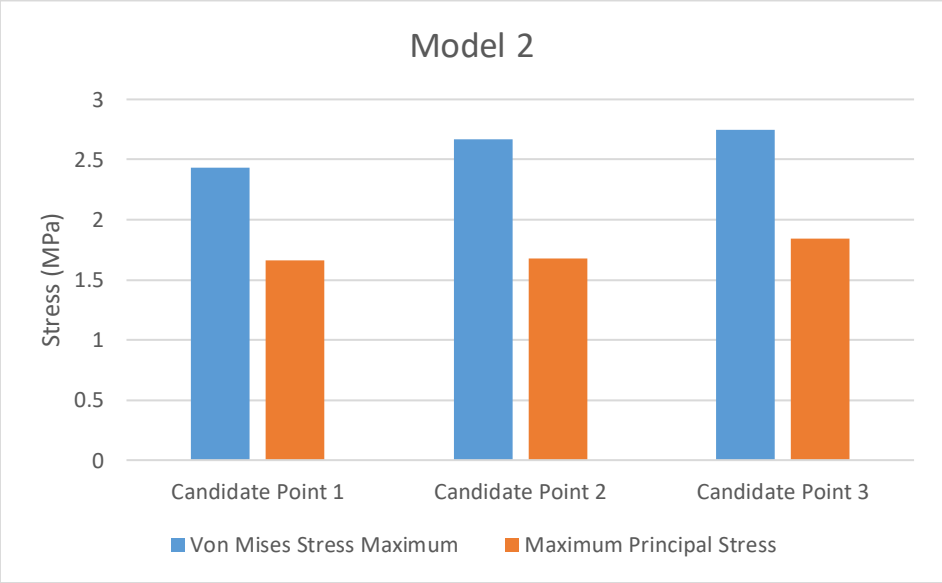

Figure 12: Comparison results Von Mises stress and Principle stress on cortical bone of Model 2.

International Journal of Engineering Research & Technology (IJERT)
ISSN: 2278-0181
Vol. 14 Issue 08, August - 2025

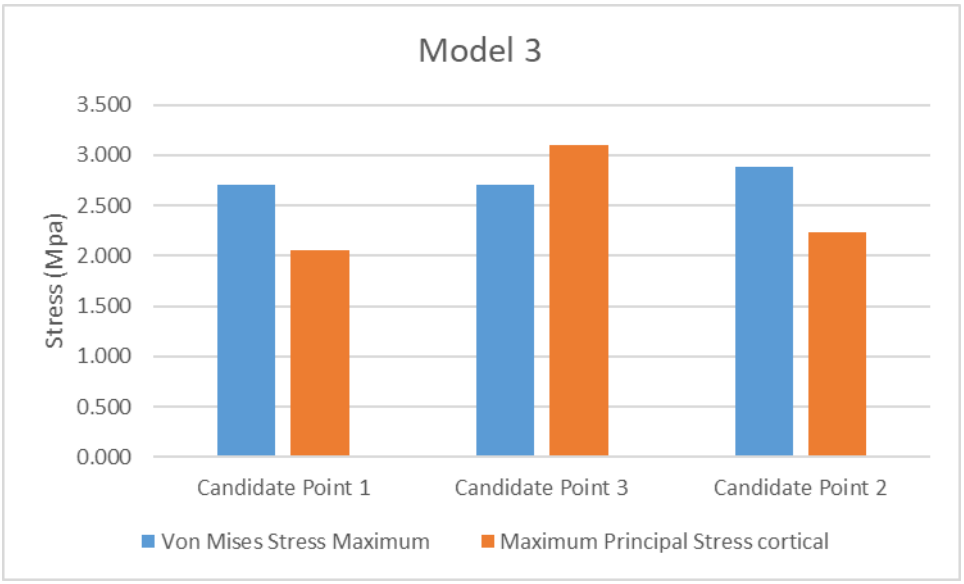

Figure 13: Comparison results Von Mises stress and Principle stress on cortical bone of Model 3.

Comparison Between Models Von-mises (Equivalent) Stress

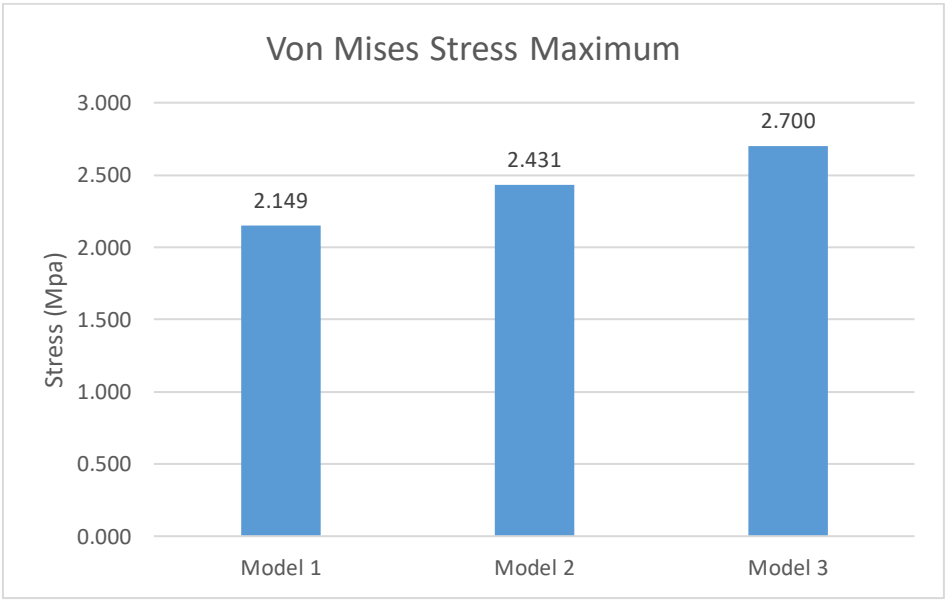

Figure 14: Comparison results Von Mises stress on cortical bone for the three models.

International Journal of Engineering Research & Technology (IJERT)
ISSN: 2278-0181
Vol. 14 Issue 08, August - 2025

Maximum Principal Stress

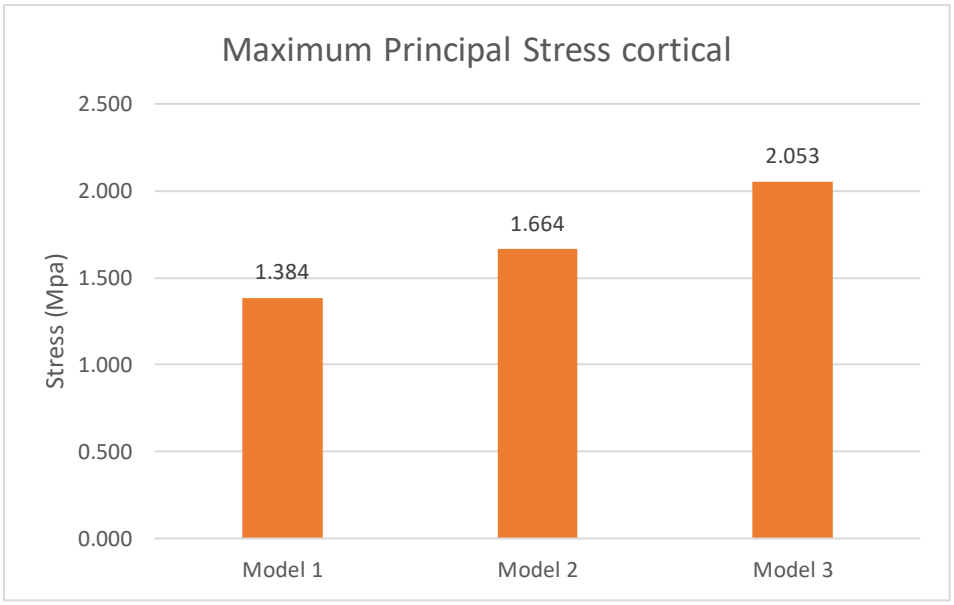

Figure 15: Comparison results Principle stress on cortical bone for the three models.

Overall Stress Comparison

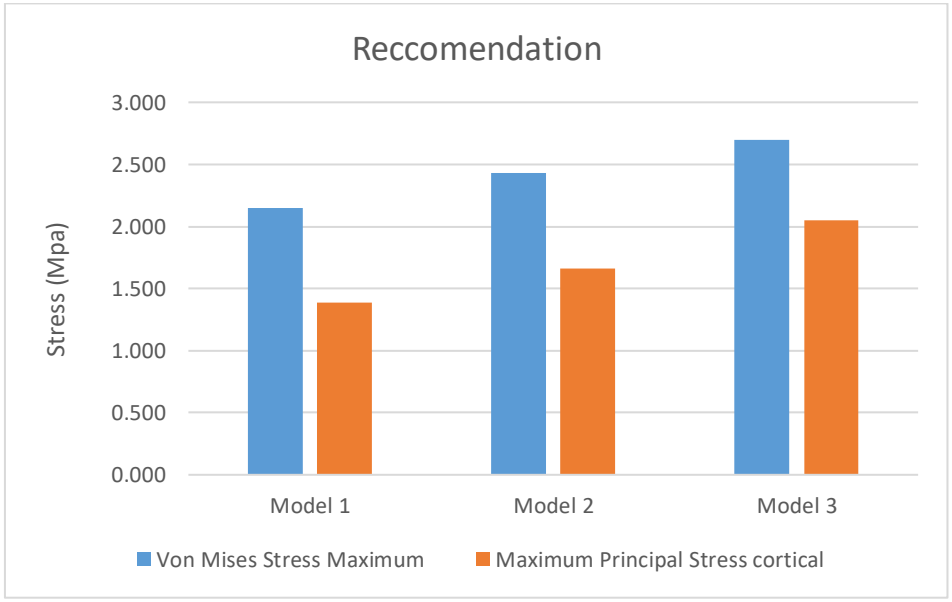

Figure 16: overall stress comparison for the three models.

International Journal of Engineering Research & Technology (IJERT)
ISSN: 2278-0181
Vol. 14 Issue 08, August - 2025

Posterior Inclination Angle Comparison

M1

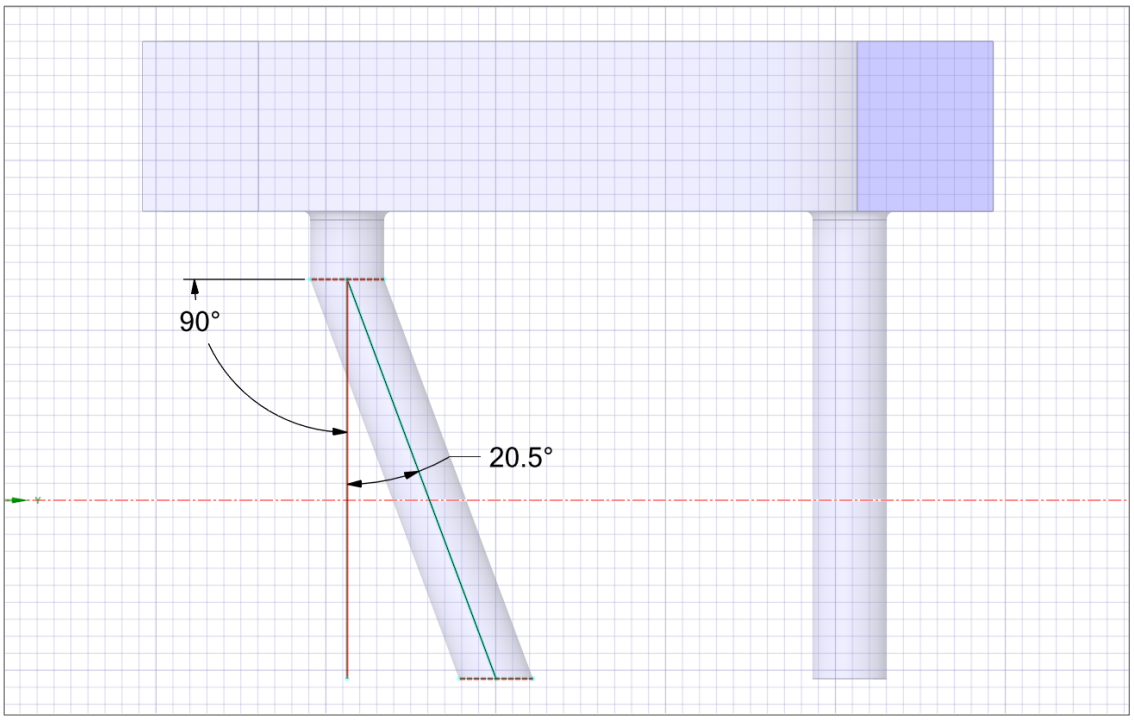

Figure 17: The posterior inclination angle for Model1.

M2

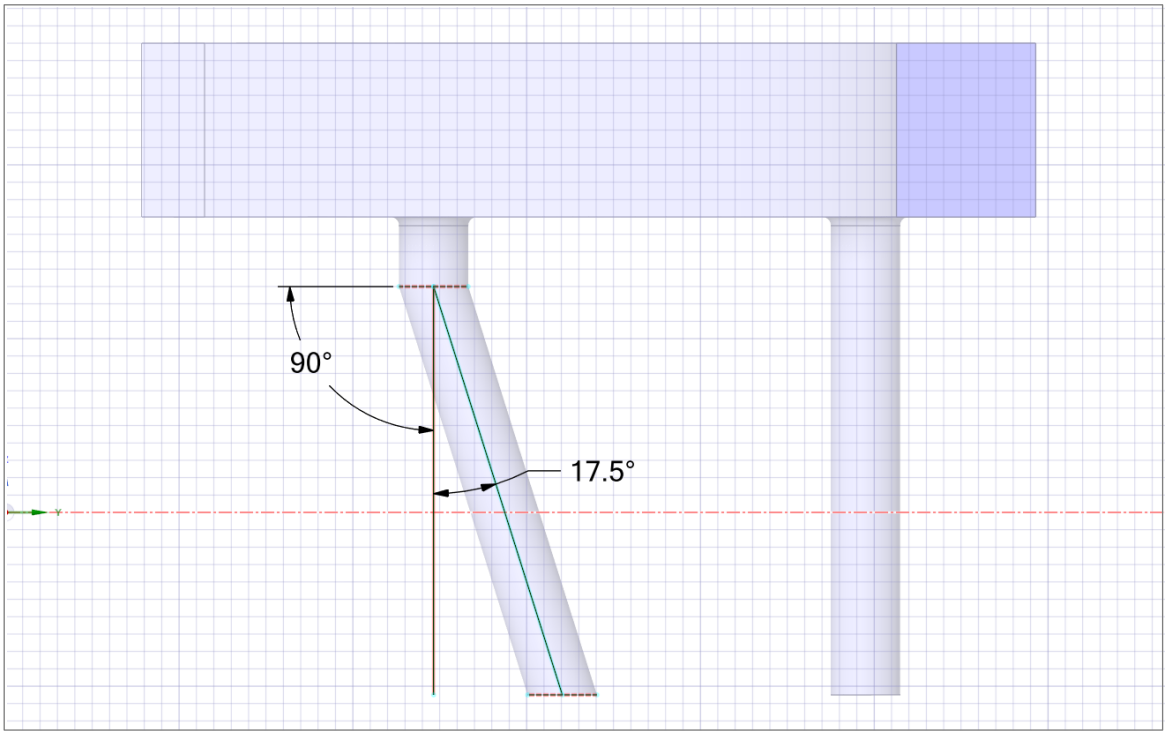

Figure 18: The posterior inclination angle for Model2.

M3

International Journal of Engineering Research & Technology (IJERT)
ISSN: 2278-0181
Vol. 14 Issue 08, August - 2025

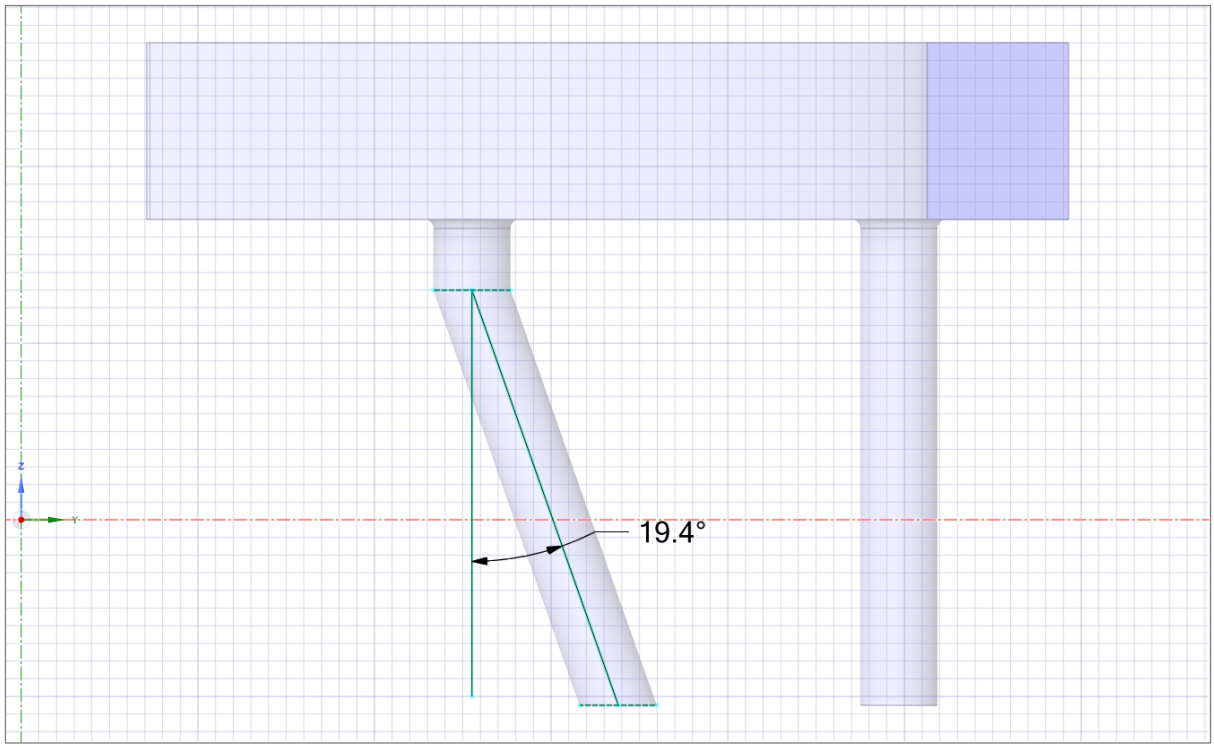

Figure 19: The posterior inclination angle for Model3.

RESULTS

Model 1 results :

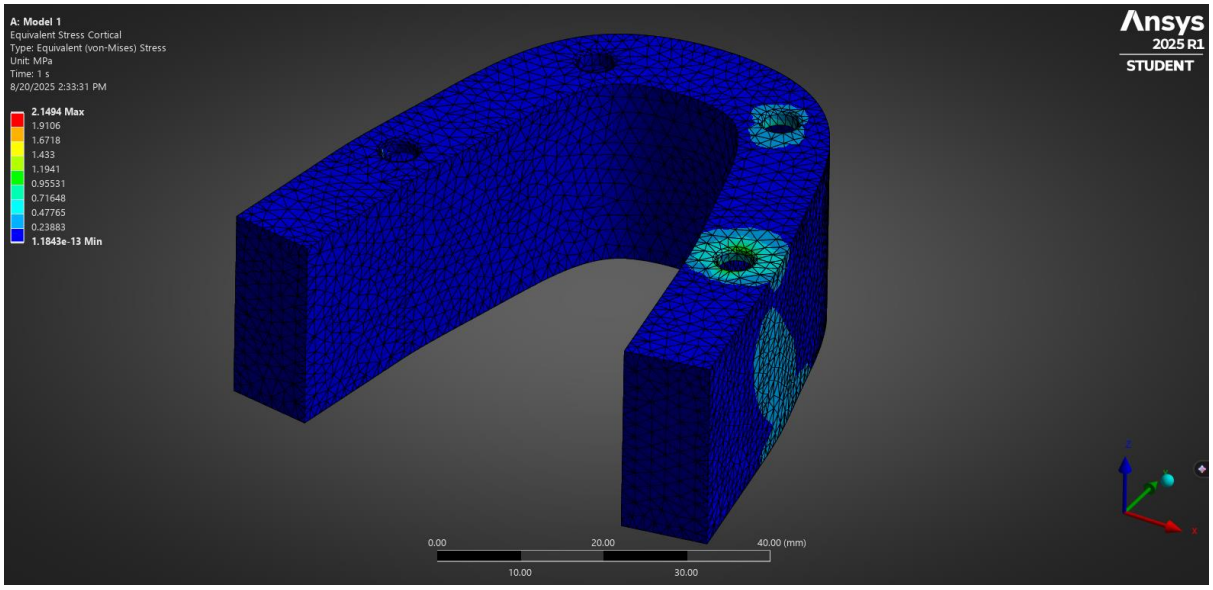

Figure 20: The maximum Von Mises equivalent stress for optimal results of Model1.

International Journal of Engineering Research & Technology (IJERT)
ISSN: 2278-0181
Vol. 14 Issue 08, August - 2025

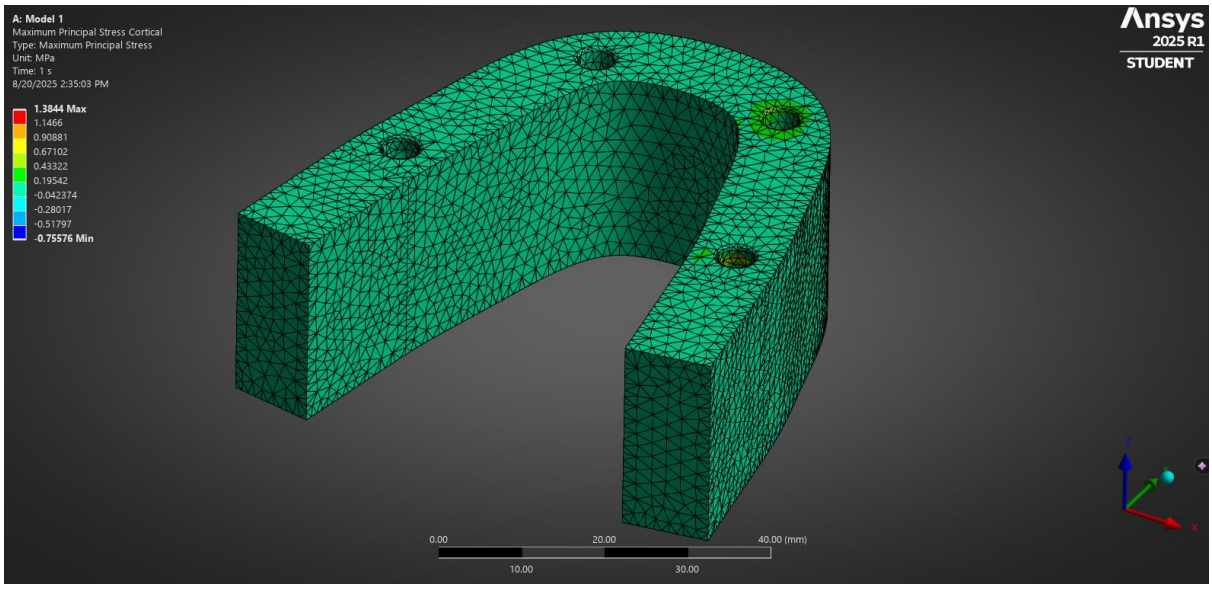

Figure 21: The maximum principal stress for optimal results of Model1.

Model 2

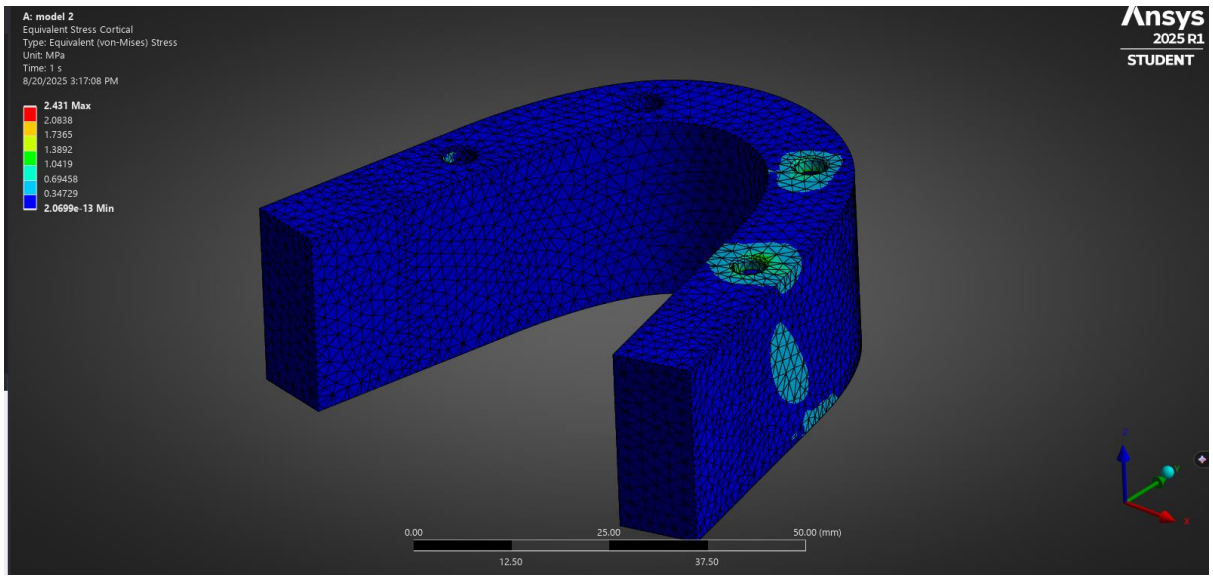

Figure 22: The maximum Von Mises equivalent stress for optimal results of Model2.

International Journal of Engineering Research & Technology (IJERT)
ISSN: 2278-0181
Vol. 14 Issue 08, August - 2025

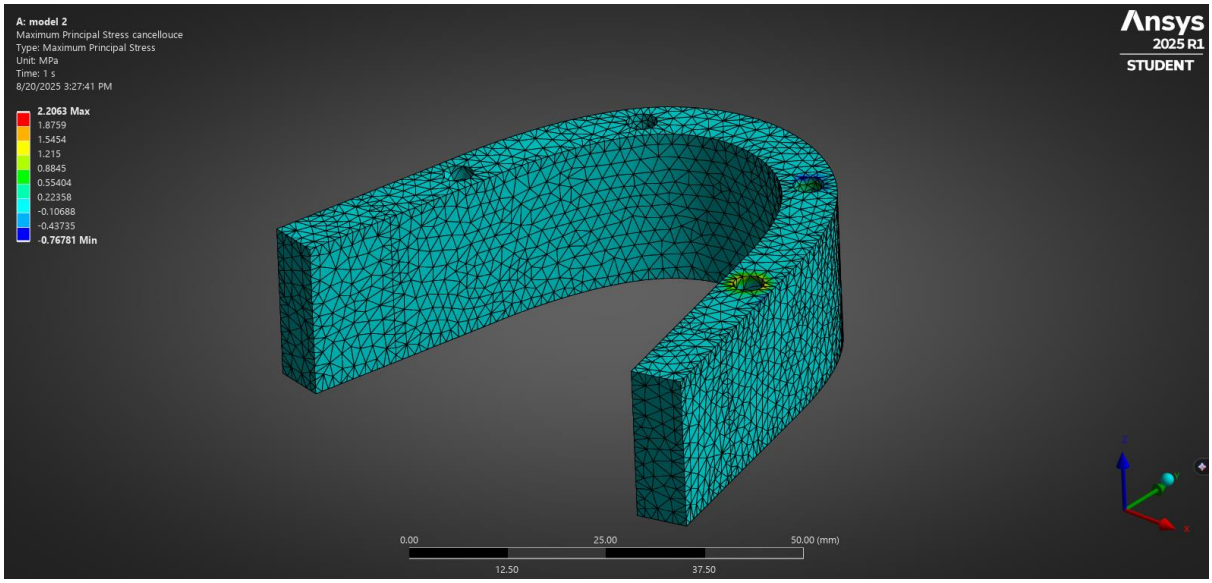

Figure 23: The maximum principal stress for optimal results of Model2.

Model 3

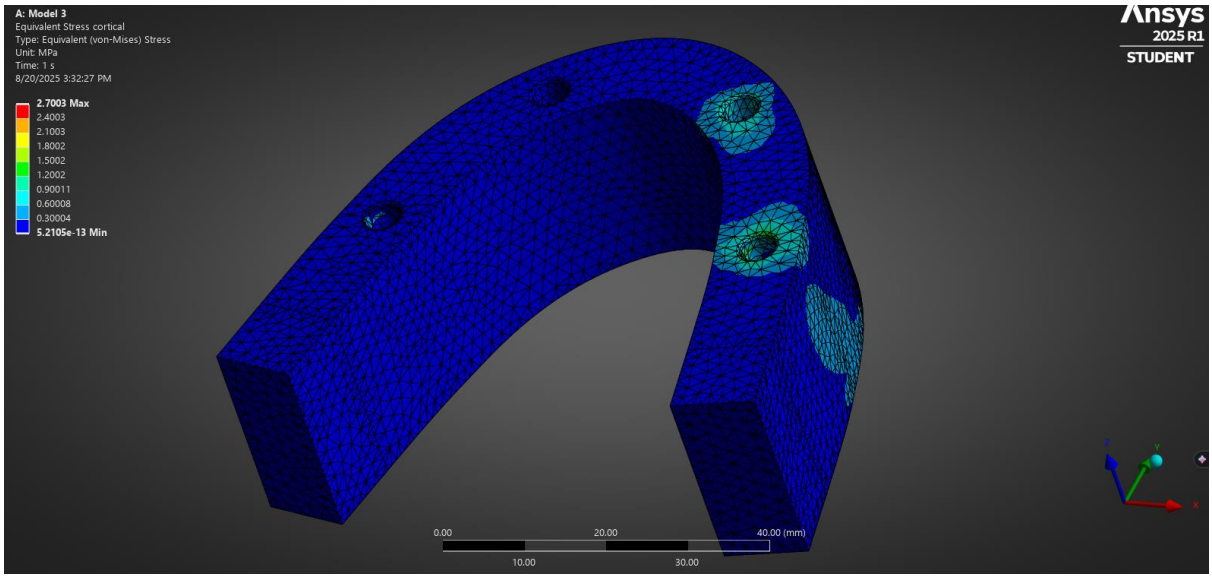

Figure 24: The maximum Von Mises equivalent stress for optimal results of Model3.

International Journal of Engineering Research & Technology (IJERT)
ISSN: 2278-0181
Vol. 14 Issue 08, August - 2025

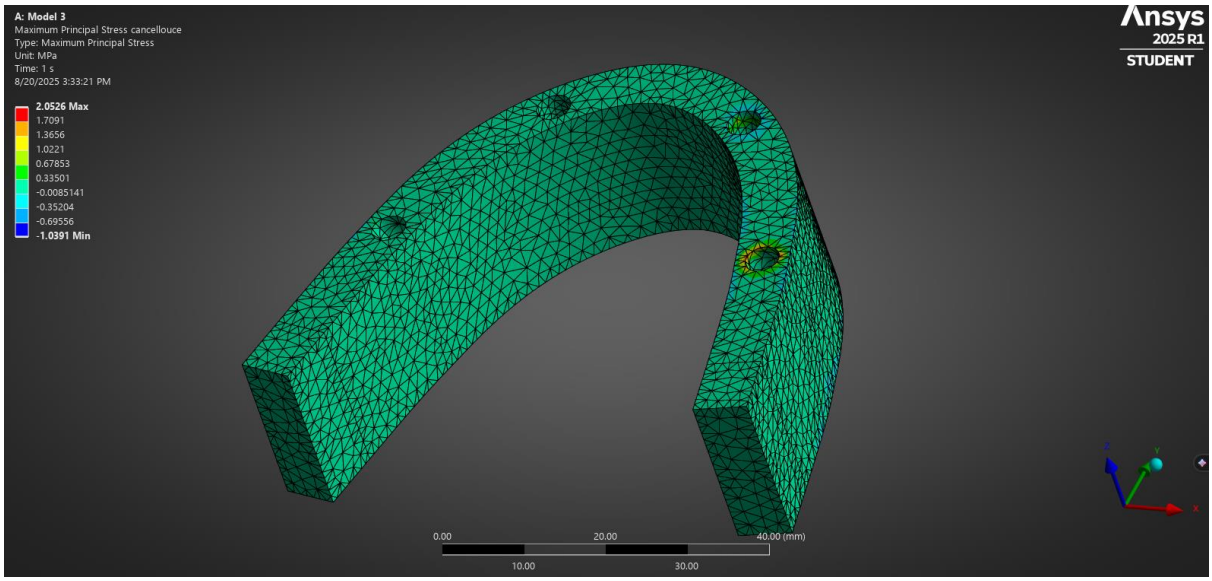

Figure 25: The maximum principal stress for optimal results of Model3.

Table 8: Summary of Optimized Candidates.

Model (Jaw Shape)	Posterior implant position angle(Degree)	Inclination Angle (Degree)	Anterior implant position angle(Degree)	Implant diameter (mm)	Von Mises Maximum	Maximum Principal Stress
Model 1 (Square)	47.699	20.5	14.163	4.355	2.149	1.384
Model 2 (Oval)	44.519	17.5	15.572	3.988	2.431	1.664
Model 3 (Tapered)	45.662	19.4	14.857	4.374	2.700	2.053

All three models returned Von Mises stress lower than 3 MPa Figures 20,22,and 24. The three models follow a clear trend with model 1 (Square) having the lowest Von mises stress value followed by model 2 (Oval) followed by model 3 (Tapered) having the highest among the three (2.1, 2.4, 2.7 MPa respectfully) Table 8 .
Implant diameter converged toward the center-to-upper bound range (4.0–4.4 mm). The best candidates cluster between ≈ 4.0–4.38 mm, often near the upper bound Table 8.
Posterior position angle (controls posterior implant position and inclination) clusters around ≈45° for the lowest stresses; angles substantially above ~50° tended to increase cortical stress Table 8.
Anterior angle (controls position of vertical anterior implants) clustered close to the median value of 15 with candidates mostly between ≈14.1–15.5° Table 8.
For each model the set of three candidate points (Tables 5-7) maintained the same ranking (square model candidate points lower than oval candidates, which were lower than tapered candidates for Von mises stress), suggesting consistent shape-dependent effects.
Maximum principal stresses followed the same ordering trend as von Mises (square lowest, tapered highest) Figures 21,23, and 25.

International Journal of Engineering Research & Technology (IJERT)
ISSN: 2278-0181
Vol. 14 Issue 08, August - 2025

DISCUSSION

Mechanical interpretation of shape based trend: square performed best and tapered worst. It is possible that the square jaw geometry provides a larger cortical support area and shorter effective lever arms for implant loads, distributing loads more evenly into the bone and reducing stress concentrations in cortical bone. The tapered (narrow) geometry reduces the available cortical envelope and increases bending moments transferred to cortical regions around the implant neck, producing higher von Mises values.

The fact that all candidate points for Model 1 are lower than those (in von mises stress) for Model 2 and Model 3 (and similarly for the other pairwise comparisons) indicates **strong shape-driven effects** rather than random optimization variation. Repeated convergence to similar optimum diameters and posterior angles across models supports the mechanical interpretations.

Diameter effect. Increased implant diameter (values trending toward ~4.0–4.4 mm) reduces local stress in the cortical bone by increasing the implant–bone contact area and effectively lowering local contact pressure and bending-induced stress concentrations. This is a consistent mechanical response: a larger cross-section reduces stress for the same applied load and bending moment.

The posterior implant position around ≈45° produced the lowest cortical stresses. Mechanically, moderate inclination reduces unfavorable cantilever moments and may improve load sharing between anterior and posterior supports. As the posterior angle increases beyond 50, inclination may create larger axial and bending moment at the cortical interface concentrating stress and raising von mises. Thus, an optimal mid ranger inclination of 50°, inclination creates larger axial components that increase bending moment at the cortical interface, concentrating stress and raising von Mises values. Thus there is an optimal mid-range posterior implant position ≈45° is sought.

Anterior angle (position) likely have limited effect. The anterior implants are vertical and their angular control parameter essentially controls position rather than any inclination. Because they are vertical and away from the load application region they do not directly cause high stresses at their bone-implant interface. They may be providing a stabilizing effect in the optimization for the geometry due to the specific loading case. Had this been a fixed parameter it could possibly cause unexpected spike of stress at the inclined implant region due to poor relative position to the inclined posterior implant. Changes in the anterior implant position are limited with candidates mostly staying within the range 14.1 to 15.5 which is around the median(of the given range).

CONCLUSION

This study used direct optimization (Ansys MOGA) to minimize cortical von Mises (and maximum principal) stress for an all-on-four denture across three Saudi jawbone morphologies (square, oval, tapered). Key conclusions:

1. Jaw shape matters. Square jaw geometry consistently produced the lowest cortical stresses (≈1.9 MPa), while tapered (narrow) geometry gave the highest (≈2.7 MPa). The shape-driven differences were consistent across candidate points, indicating robust geometric influence on stress distribution.

2. Implant diameter should be as large as anatomically feasible. All models converged toward implant diameters near the upper bound (≈4.0–4.4 mm), indicating larger diameters reduce cortical stress by improving load distribution.

3. Posterior implant inclination has an optimal mid-range (~45°). Posterior angles ≈45° minimized cortical stress; higher inclinations (>~50°) tended to increase cortical stress due to larger bending moments.

4. Anterior implant position had limited effect in the tested range. Small variation in anterior positional angle (13.5–16.5°) produced little change in cortical stress compared to diameter and posterior inclination effects.

International Journal of Engineering Research & Technology (IJERT)
ISSN: 2278-0181
Vol. 14 Issue 08, August - 2025

This study concludes that the stress distribution within the cortical bone is significantly influenced by four key factors: the fit of the all-on-four model to the patient's specific mandibular shape, the strategic placement of implants along the mandibular curvature, the patient-specific degree of posterior implant inclination, and the implant diameter. These results underscore the necessity of adopting a customized design strategy based on precise jaw specifications, including morphology, bone density, and the calculated determination of optimal implant position and angulation.

REFERENCE1

[1] "Dental arch dimensions, form and tooth size ratio among a Saudi sample - PMC." Accessed: Aug. 27, 2025. [Online]. Available: https://pmc.ncbi.nlm.nih.gov/articles/PMC5885126/

[2] T. Takahashi, I. Shimamura, and K. Sakurai, "Influence of number and inclination angle of implants on stress distribution in mandibular cortical bone with All-on-4 Concept," *J. Prosthodont. Res.*, vol. 54, no. 4, pp. 179–184, Oct. 2010, doi: 10.1016/j.jpor.2010.04.004.

[3] P. Maló, B. Rangert, and M. Nobre, "'All-on-Four' Immediate-Function Concept with Brånemark System® Implants for Completely Edentulous Mandibles: A Retrospective Clinical Study," *Clin. Implant Dent. Relat. Res.*, vol. 5, no. s1, pp. 2–9, 2003, doi: 10.1111/j.1708-8208.2003.tb00010.x.

[4] N. Asawa, N. Bulbule, D. Kakade, and R. Shah, "Angulated Implants: An Alternative to Bone Augmentation and Sinus Lift Procedure: Systematic Review," *J. Clin. Diagn. Res. JCDR*, vol. 9, no. 3, pp. ZE10–ZE13, Mar. 2015, doi: 10.7860/JCDR/2015/11368.5655.

[5] "Contemporary 'All-on-4' Concept - Dental Clinics." Accessed: Aug. 26, 2025. [Online]. Available: https://www.dental.theclinics.com/article/S0011-8532(14)00157-8/abstract

[6] "The All-on-Four Treatment Concept: A Systematic Review - Patzelt - 2014 - Clinical Implant Dentistry and Related Research - Wiley Online Library." Accessed: Aug. 26, 2025. [Online]. Available: https://onlinelibrary.wiley.com/doi/abs/10.1111/cid.12068

[7] G. Deste and R. Durkan, "Effects of all-on-four implant designs in mandible on implants and the surrounding bone: A 3-D finite element analysis," *Niger. J. Clin. Pract.*, vol. 23, no. 4, pp. 456–456, Apr. 2020.

[8] S. Vladimir, "Review Article on the All-On-Four Treatment Concept in Dental Implants," *Arch. Surg. Clin. Res.*, vol. 7, no. 2, pp. 019–023, July 2023, doi: 10.29328/journal.ascr.1001070.

[9] P. Thumati, M. Reddy, M. Mahantshetty, and R. Manwani, "'All-On-4/DIEM 2' A concept to rehabilitate completely resorbed edentulous arches," *J. Dent. Implants*, vol. 5, no. 1, p. 76, June 2015, doi: 10.4103/0974-6781.154455.

[10] B. Anandh, B. Lokesh, V. Ebenezer, S. Jimson, and J. Parthiban, "All on Four – The Basics," *Biomed. Pharmacol. J.*, vol. 8, no. October Spl Edition, pp. 609–612, Oct. 2015.

[11] O. C. Thiele *et al.*, "Craniomaxillofacial patient-specific CAD/CAM implants based on cone-beam tomography data – A feasibility study," *J. Cranio-Maxillofac. Surg.*, vol. 46, no. 9, pp. 1461–1464, Sept. 2018, doi: 10.1016/j.jcms.2018.05.056.

[12] "Finite Element Assessment of a Novel Patient-Specific Mandibular Implant for Severely Atrophic Ridge - Parhiz - 2024 - BioMed Research International - Wiley Online Library." Accessed: Aug. 26, 2025. [Online]. Available: https://onlinelibrary.wiley.com/doi/full/10.1155/2024/9735427

[13] "Biomechanical Investigation of Patient-Specific Porous Dental Implants: A Finite Element Study." Accessed: Aug. 26, 2025. [Online]. Available: https://www.mdpi.com/2076-3417/13/12/7097

[14] B. B. J. Merema, J. Kraeima, H. H. Glas, F. K. L. Spijkervet, and M. J. H. Witjes, "Patient-specific finite element models of the human mandible: Lack of consensus on current set-ups," *Oral Dis.*, vol. 27, no. 1, pp. 42–51, 2021, doi: 10.1111/odi.13381.

[15] M. H. Chan and C. Holmes, "Contemporary 'All-on-4' Concept," *Dent. Clin.*, vol. 59, no. 2, pp. 421–470, Apr. 2015, doi: 10.1016/j.cden.2014.12.001.

[16] A. Y.-J. Wu, J.-T. Hsu, W. Chee, Y.-T. Lin, L.-J. Fuh, and H.-L. Huang, "Biomechanical evaluation of one-piece and two-piece small-diameter dental implants: In-vitro experimental and three-dimensional finite element analyses," *J. Formos. Med. Assoc.*, vol. 115, no. 9, pp. 794–800, Sept. 2016, doi: 10.1016/j.jfma.2016.01.002.

[17] "Characteristics of Mandibular Arch Forms in Patients with Skeletal Mandibular Prognathism." Accessed: Aug. 26, 2025. [Online]. Available: https://www.mdpi.com/2075-4418/13/20/3237

[18] M. H. Saleh, "Arch Dimensions Changes of Egyptian Orthodontic Patients using Different Orthodontic Archwires: A Prospective Clinical Study," vol. 6, no. 10.

[19] "Dental Arch Dimensions in Saudi Adults - Alkadhi - 2018 - International Journal of Dentistry - Wiley Online Library." Accessed: Aug. 26, 2025. [Online]. Available: https://onlinelibrary.wiley.com/doi/full/10.1155/2018/2190250

[20] T. Kanchan, V. Chugh, A. Chugh, P. Setia, R. Shedge, and K. Krishan, "Estimation of Sex From Dental Arch Dimensions: An Odontometric Analysis," *J. Craniofac. Surg.*, vol. 32, no. 8, p. 2713, Dec. 2021, doi: 10.1097/SCS.0000000000007787.

[21] M. A. Ali and Y. A. Yassir, "Mandibular Clinical Arch Forms in Iraqi Population: A National Survey," *Diagnostics*, vol. 12, no. 10, p. 2352, Oct. 2022, doi: 10.3390/diagnostics12102352.

[22] M. M. A. Moaleem *et al.*, "Analysis of the Facial Measurements and Dental Arch Dimensions for the Construction of Dental Prostheses among Adult Yemenis," *J. Contemp. Dent. Pract.*, vol. 24, no. 8, pp. 595–604, Sept. 2023, doi: 10.5005/jp-journals-10024-3511.

[23] "Maxillary and mandibular dental arch forms in a Jordanian population with normal occlusion | BMC Oral Health." Accessed: Aug. 26, 2025. [Online]. Available: https://link.springer.com/article/10.1186/s12903-021-01461-y

[24] S. Gupta, R. Fernandes, S. Natarajan, N. P. Jose, J. Giri, and S. Dahal, "Comparative evaluation of arch form among the Nepalese population: A morphological study," *J. Oral Maxillofac. Pathol.*, vol. 28, no. 1, p. 111, Mar. 2024, doi: 10.4103/jomfp.jomfp_280_23.

[25] C. S. López, C. H. Saka, G. Rada, and D. D. Valenzuela, "Impact of fixed implant supported prostheses in edentulous patients: protocol for a systematic review," Feb. 2016, doi: 10.1136/bmjopen-2015-009288.

[26] "Subjective and objective evaluation of masticatory function in patients with bimaxillary implant-supported prostheses - Homsi - 2023 - Journal of Oral Rehabilitation - Wiley Online Library." Accessed: Aug. 26, 2025. [Online]. Available: https://onlinelibrary.wiley.com/doi/full/10.1111/joor.13393

International Journal of Engineering Research & Technology (IJERT)
ISSN: 2278-0181
Vol. 14 Issue 08, August - 2025

[27] A. Moeintaghavi, A. S. Madani, and M. Rezaeei, "Occlusal Rehabilitation in a Partially Edentulous Patient with Lost Vertical Dimension Using Dental Implants: A Clinical Report," *J. Contemp. Dent. Pract.*, vol. 11, no. 6, pp. 58–64, Sept. 2008, doi: 10.5005/jcdp-11-6-58.
[28] A. Al Baker, S. R. Habib, and M. D. Al Amri, "Preserving esthetics, occlusion and occlusal vertical dimension in a patient with fixed prostheses seeking dental implant treatment," *Saudi Dent. J.*, vol. 28, no. 4, pp. 203–208, Oct. 2016, doi: 10.1016/j.sdentj.2016.05.003.
[29] F. Ebrahimi, *Finite Element Analysis: New Trends and Developments*. BoD – Books on Demand, 2012.